STUDYING AND ELIMINATING ADVENTITIOUS CARBON CONTAMINATION ON SILICON WAFERS

by

Elisabeth Strein

A senior thesis submitted to the faculty of

Brigham Young University

in partial fulfillment of the requirements for the degree of

Bachelor of Science

Department of Physics and Astronomy

Brigham Young University

August 2008

Copyright © 2008 Elisabeth Strein

All Rights Reserved

BRIGHAM YOUNG UNIVERSITY

DEPARTMENT APPROVAL

of a senior thesis submitted by

Elisabeth Strein

This thesis has been reviewed by the research advisor, research coordinator, and department chair and has been found to be satisfactory.

Date	David Allred, Advisor
Date	Eric Hintz, Research Coordinator
Date	Ross Spencer, Chair

ABSTRACT

STUDYING AND ELIMINATING ADVENTITIOUS CARBON CONTAMINATION ON SILICON WAFERS

Elisabeth Strein

Department of Physics and Astronomy

Bachelor of Science

Cleaning techniques for Si/SiO_2 ultrathin films are presented. With the removal of adventitious carbon on the surface, Si/SiO_2 ultrathin films can serve as calibration standards in vacuum ultraviolet reflectance characterization (the range from 8 to 60 nm). Our group anticipates using these standards when making a mirror that will be sent to the moon and will be used to study the earth's magnetosphere. Data are presented for the samples that demonstrate the elimination of adventitious carbon contamination via oxygen radicals and chemical treatments. Data are determined by x-ray photoelectron spectroscopy (XPS) and spectroscopic ellipsometry. Additionally, I found that the antechamber of the XPS system deposits hydrocarbon onto the surface of samples. I adapted a plasma cleaner so that it minimized the effects of this instrumental contamination. I found that samples must be cleaned with the lamp for at least five minutes or cleaned with the two-step chemical RCA

clean. I found a correlation between the ellipsometry data and the XPS data. Finally I stored samples and found that carbon begins to redeposit on the sample surface within 2 hours of cleaning it. Storage data are presented.

ACKNOWLEDGMENTS

I would like to acknowledge the BYU College of Physical and Mathematical Sciences and the Department of Physics and Astronomy for their financial support which made the success of this project possible. I am indebted to Gabe Morgan and Ron Vane with XEI Scientific, Inc. for their loan of an EVACTRON® C Oxygen Radical Source for our XPS system. Likewise, the following individuals aided me greatly in the XPS phase of this research: Amy Grigg, Lei Pei, and Professor Matt Linford. My deepest thanks goes to Dr. David Allred and Dr. R. Steven Turley. They have dedicated many hours towards guiding me in research and opened doors for me that have had an extraordinary impact on my undergraduate experience. A lot of my passion for research stems from the fact that I had such extraordinary advisors.

I also need to thank my roommates and my family. Without their love I never would have made it. Nor would I have survived without the support and friendship of my fellow physics undergrads. I am very grateful to Duane Merrell, John McIlmoil, and my high school students for teaching me how to communicate physics to other people. Also Mike Steigerwald at Columbia has taken such a vested interest in my life and provided outside perspective when I most needed it, I will always be grateful that he is my friend. Most of all I'd like to thank God for He played an active role in helping me with research. He inspired me when I was confused, He gave me strength when I was exhausted and His support has made me realize that my problems matter to Him.

Contents

Table of Contents **vii**

List of Figures **viii**

1 Introduction **1**

2 Details **7**
2.1 Instrumentation and Instrumentational Techniques 8
2.2 Cleaning Techniques 11

3 Results and Conclusion **14**

Bibliography **26**

A Ellipsometry **29**

List of Figures

1.1 List-of-Figs. Sample Figure 2
1.2 List-of-Figs. Sample Figure 3

2.1 Contamination from the XPS antechamber 9
2.2 Schematic of evactron installed onto the XPS antechamber 10

3.1 Cleaning results from the UV excimer lamp 15
3.2 Correction between the ellipsometry and XPS results 18
3.3 XPS survey scans 20
3.4 carbon comparison between dirty and clean samples 21
3.5 Peaks for C (*1s*) from XPS 22
3.7 Comparison of carbon peaks for RCA cleaned and lamp cleaned . . . 23
3.8 Growth in apparent oxide thickness after the RCA clean 24
3.9 Storage data results 25
3.10 Storage data results 25

A.1 diagram of how s and p polarized light reflects 30
A.2 possible paths for the light at the first boundary 32
A.3 variation in Brewster's angle for silicon for the wavelengths measured with the ellipsometer 36

Chapter 1

Introduction

In 1998 BYU's EUV/thin film group made a set of EUV (30.4 nm) mirrors for the IMAGE space craft which was launched 25 March 2000 and circled the earth studying the earth's magnetosphere. Our group anticipates making another mirror because several groups in the US and in China are contemplating sending Earth-observing telescopes to the moon. The moon mirror would be used with other instruments to map the earth's magnetosphere by imaging the ionized helium caught in it.

We can image the ionized helium because radiation from the sun reflects from it, causing a spectral line at 30.4 nm. We will design the aperiodic-multilayer mirror to cause constructive interference at this wavelength. A second design criterion is to force deconstructive interference at 58.4 nm, where there is a bright spectral line created by that neutral helium found throughout the solar system. The spectral line at 58.4 nm is so strong that without this deconstructive interference, the line at 30.4 nm is washed out and is impossible to image.

The two wavelengths of interest fall into the extreme ultraviolet range of the spectrum. This is a challenging energy range in which to make reflection measurements. Surface contamination has a dramatic effect on reflection. This can be demonstrated

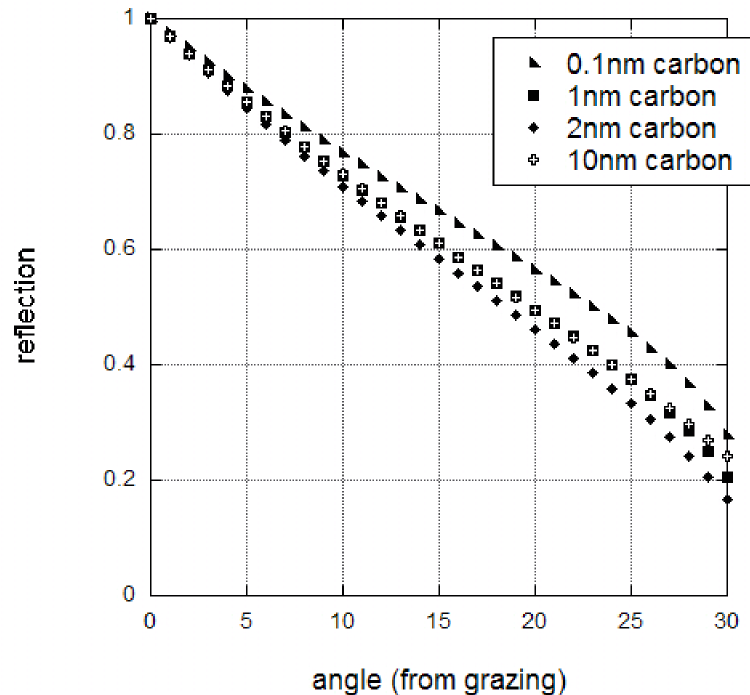

Figure 1.1 Calculated reflectance for 41.3nm (30eV) light on a silicon wafer with an oxide that is 1.8nm thick. The reflectance decreases as the adventitious carbon on the surface increases. [1] [2]

with both theoretical calculations(see Fig. 1.1) and experimental data (see Fig. 1.2). The experimental data comes from work done at NASA in the late 90s. They compared reflection from two mirrors that both initially show high reflection from wavelengths ranging from 120 to 150 nm. One mirror was left in high vacuum at $\leq 1\times10^{-7}$ Torr, the other found was contaminated with 2 nm of Hysol epoxy and photopolymerized for 3.5 hours. Figure 1.2 demonstrates that surface contamination dramatically reduces reflectivity at these wavelengths. The effects of organic contamination will be all the more pronounced for our mirror since it will be designed for wavelengths between 30 to 60 nm. The theoretical calculations at 41 nm show that even 1nm of organic contamination changes the reflectivity of the sample.

Granted, once the mirror is on the moon, organic (adventitious carbon) contamination from the ambient air will no longer be an issue, but during the process of

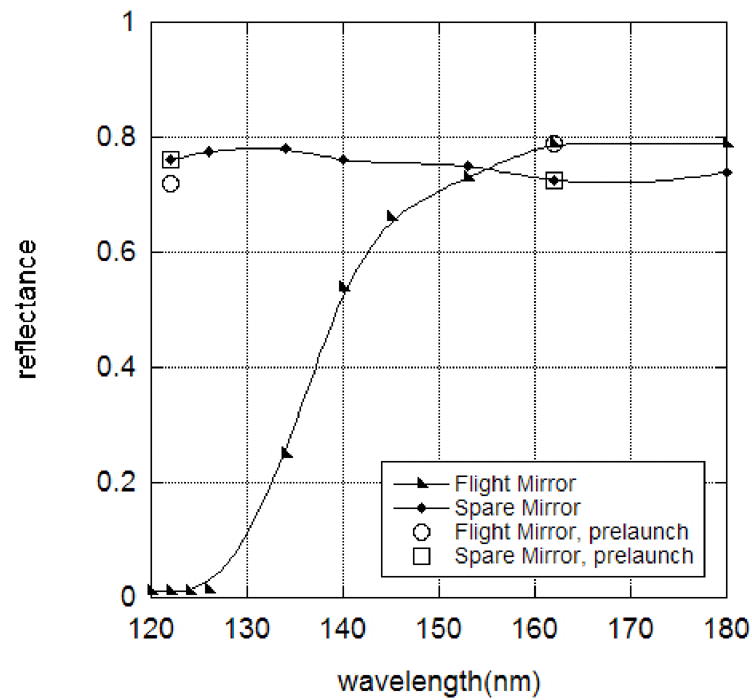

Figure 1.2 In 1999 NASA reported that surface contamination on EUV mirrors dramatically decreased the mirror's reflectivity. Their data shows the drastic difference in EUV reflectance between a mirror that was exposed to adventitious carbon and one that was not. [3]

making, characterizing, shipping, storing, and launching it is critical that we understand this unavoidable contamination. Furthermore, contamination elimination has applications for work beyond our moon mirror. For us to make meaningful contributions towards determining optical constants in the EUV (which is the principal goal of our group), we must have extremely accurate data in order for the third and fourth decimal places of our calculated constants to be believable. Contamination elimination is therefore critical. Finally, returning to the moon mirror project, in order to make meaningful reflectance measurements with it, we must have calibration standards to compare with the mirror. The work of this thesis focuses specifically on cleaning and storing such a standard–a thermally grown oxide on silicon. Since the presence of adventitious carbon changes the way silicon reflects in the EUV (see Fig. 1.1), we need to ensure that apparent oxide on a silicon wafer is clean, stable, smooth, and well characterized. Hyrdocarbon contamination needs to be eliminated. Furthermore, we also need to assure that the surface of the mirror is smooth. Roughness grossly decreases reflectance [4]. Thus, my aim was to study cleaning processes that would eliminate advenitious carbon while maintaining a smooth surface.

Many people are aware of problems associated with hydrocarbon thin films in because in the semiconducting industry they arise during device fabrication. For example, organic contamination can mask surfaces causing poor adhesion when attempting to deposit layers. Hydrofluoric acid (HF) is commonly used to ensure that a surface is atomically clean. For our mirror however, HF is not a viable option because it would eliminate oxide on the mirror and the standard [5]. Another technique commonly used in industry is the RCA clean This option is a wet chemistry cleaning procedure that cleans hydrocarbon contamination while preserving the oxide layer. The results of this technique were compared extensively with the results of cleaning with a xenon excimer lamp. I also briefly studied cleaning via two versions of plasma

cleaners, a Harrick plasma cleaner and an Evactron plasma cleaner. The lamp and both plasma cleaners use oxygen radicals to oxidize the hyrocarbons and form volatile oxide products. Due to their voltality, the oxide products interact with the carbon, thus freeing the surface of organics.

I studied the effects of various cleaning treatments primarily with mulitwavelength ellipsometry and with X-ray photoelectron spectroscopy (XPS)[1]. In addition to cleaning the samples I had to ensure that my analysis didn't cause further contamination to my surfaces. One of the plasma cleaners, the Evactron C, was tremendously useful in eliminating contamination inside the XPS antechamber that deposited onto the surface of the samples before I was able to analyze them. I regularly used the Evactron plasma cleaner to clean the chamber prior to putting my samples in it. I concluded that both the RCA clean and five to six minutes under the excimer lamp eliminate a similar amount of carbon. The RCA leaves a thinner oxide layer than the lamp. The Harrick plasma cleaner deposits a significant amount of fluorine on the surface of samples but does an excellent job of rapidly eliminating carbon. The Evactron plasma cleaner appears to eliminate carbon but at a much slower rate than the other cleaning methods. It is better used as a way to clean the chamber rather than a way to clean the samples.

In addition to studying ways of eliminate surface contamination while preserving the oxide layer and minimizing surface roughness, I also studied different ways of storing samples and looked at how quickly carbon contamination returns. I found that even within the best storage conditions, for both the excimer lamp and the RCA clean,

[1]Occasionally I used the contact angle to verify that a sample had been contaminated. Clean samples had a strongly hydrophilic surface: the droplet completely spread out and the contact angle was very close to 0. Contaminated samples were still hydrophilic but less so then the cleaned ones. Measuring the contact angle proved particularly useful when I had conflicting results from ellipsometry and XPS.

after two hours of being cleaned, the apparent oxide thickness consistantly grew by 0.1 to 0.2 nm. We presume that the majority of this growth is attributed to advenitious carbon redepositing on the surface. Contamination accumulation over time occurs on all samples but the growth is the most pronounced for samples that have been recently cleaned. Over the long term cleaned samples will generally accumulate more contamination than samples that were left untouched.

This thesis will discuss the details of the cleaning methods I used. It will discuss the results of the cleaning and storage studies. I will discuss the details of cleaning methods, the Evactron and its role in this research, and the details of storing the samples. In the appendix I present the theory and fitting done by the ellipsometer.

Chapter 2

Details

In this chapter I will discuss my experimental work. In first section I present the details of the equipment and instruments I used in this research. I will describe the samples. I will also describe the two instruments I used to characterize samples (XPS and the ellipsometer)and the two cleaning instruments I used to minimize adventitious carbon contamination. For the vast majority of the studies, either the RCA clean or the excimer lamp was used to clean samples and the Evactron plasma cleaner was used to clean contamination in the XPS antechamber. In the second section I will detail the cleaning procedures and equipment that I used. Control samples were established with samples that were not exposed to any cleaning treatment. They were characterized alongside the cleaned samples, using the same techniques and instrumentation. Most experiments were repeated at least three times to ensure the repetition of results.

2.1 Instrumentation and Instrumentational Techniques

I cleaned silicon samples cleaved from [1,0,0] silicon wafers. Prior to cleaning, these wafers were stored in a variety of conditions; however, the vast majority of them were cut from wafers that were stored vertically in the original factory packaging. All samples started with an apparent oxide thickness of at least 2.1 nm and with an average thickness of 2.27±0.15 nm for 55 samples. I aimed to eliminate the adventitious carbon on the surface of the SiO_2 thus creating a silicon substrate capped only with the native oxide layer (approximately 1.8 nm thick).

I used a J.A. Woollam spectroscopic ellipsometer (M2000) to detect a change in thickness in the apparent oxide layer. Since we were interested in carbon elimination it would seem more intuitive to measure the thickness of the adventitious carbon layer on top of the oxide. It is, therefore, important to understand why I measured the apparent oxide layer. Typically, the layer of adventitious carbon was thin enough that the ellipsometer (using wavelengths of light from 191.72 to 989.29 nm) could not distinguish a difference between the oxide and the carbon. However, despite the ellipsometer's inability to detect a carbon layer, I detected carbon with x-ray photoelectron spectroscopy (XPS). I was able to get the ellipsometer to "detect" the carbon with back-door modeling: I modeled the samples using an "oxide layer" on top of a silicon substrate. The carbon-oxide layer change the polarization of the light and from that change the WAVE program calculates a thickness for that "layer." After I cleaned the samples, I again used the ellipsometer to determine the new thickness of the "oxide" layer. The "thickness" of the adventitious carbon layer is the difference between the two thicknesses. Finally I used XPS to confirm that the decrease in the apparent oxide thickness corresponded with a decrease in the carbon to silicon ratio.

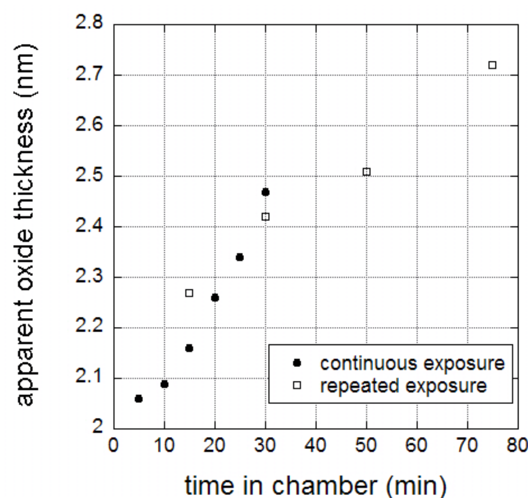

Figure 2.1 Apparent oxide layer vs time in the XPS antechamber. Note that samples which spent the same amount of time in the chamber don't necessarily experience the same rate of carbon growth. Samples that were repeatedly exposed to the chamber show a marked difference in the growth rate from the samples that were exposed for one continuous run.

For more information as to how an ellipsometer works and how the data it collects is correlated with a thickness measurement, please refer to the appendix.

For this research, x-ray photoelectron spectroscopy characterization was preformed by a SSX-100 ESCA Spectrometer with a conventional Al Kα anode. All measurements were taken at better than 2×10^{-8} Torr. The system was regularly calibrated using the principal peaks for copper and gold. Binding energies were referenced based on this calibration. In my use of this instrument, I discovered that the XPS antechamber was a source of substantial carbon contamination. Before samples could be introduced into the main chamber, the operating procedure dictated that they needed to wait at least 30 minutes in the antechamber while it pumped down before they could be introduced into the high vacuum environment of the main chamber. Through XPS I observed a significant carbon presence. Using ellipsometry measurements taken before and after chamber exposure I determined that the apparent oxide layer grew 0.6 nm after it was exposed to the chamber for 30 minutes while one that was cleaned and left in air grew by less than one angstrom (see Fig. 2.1). Furthermore,

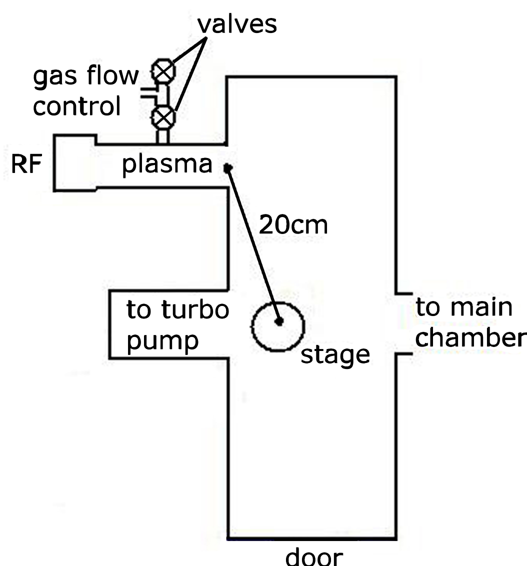

Figure 2.2 Schematic of the XPS antechamber with the addition of the Evactron system. The volume of the antechamber is 22L.

after about ten minutes of being in the chamber the growth became linear and grew at a rate of 0.02 nm/min. This discovery necessitated the use of an Evactron® C De-Contaminator RF Plasma Cleaning System. This device was designed to remove hydrocarbon contamination from Scanning Electron Microscope (SEM) chambers via neutral oxygen radicals. The Evactron follows the basic operating principles of plasma ashing, a standard technique for removing a photoresist in semiconductor manufacturing. It creates oxygen radicals that oxidize the hydrocarbon contamination and combine with the adventitious carbon in the chamber. These new oxides are then removed by the antechamber's turbo pump. For a diagram of how the Evactron was integrated onto the XPS system please see fig 2.2. In principle, hydrocarbon contamination could also be eliminated by baking the antechamber. The increased heat would allow oxygen molecules (rather than the oxygen *atoms* in the plasma) to oxidize the hydrocarbons. Unfortunately, the increased heat is significantly more difficult to control. The oxygen atoms created by the Evactron are more reactive than oxygen

molecules at room temperature and they provide stable and reproducible cleaning results.

The Evactron operates by using the strong electromagnetic field produced with a radio frequency (RF) potential to make a plasma. The potential accelerates oxygen molecules causing them to break apart into monatomic form. This process is called disassociation and it creates both plasma ions and neutral oxygen radicals. The plasma ions are highly reactive and can be destructive to the chamber. They are also a shorter-lived species than the neutral oxygen radicals. The Evactron takes advantage of this by creating the plasma outside the chamber so only the neutral long-lived radicals survive long enough to be introduced into the chamber. The neutral oxygen atoms introduced into the chamber oxidize the adventitious carbon and the resulting molecules are pumped out of the system.

We operated the Evactron when antechamber pressure was at 0.4 Torr. This pressure was stabilized by adjusting the flow rate from the Oxygen Radical Source (ORS) device on the Evactron to balance the pumping speed of the antechamber's turbo pump. The RF power was set at 12 Watts. We didn't find it necessary to use the optional nitrogen purge mode. For the majority of data presented in this thesis, I used the Evactron on the chamber and on the stage before I introduced the samples to them. Also I varied the time that I cleaned the chamber with the Evactron and found that as long as the chamber was relatively clean 20 minutes was sufficient.

2.2 Cleaning Techniques

As mentioned previously, silicon wafers (100 orientation) have a native oxide that is approximately 1.8 nm thick. My goal was to free the wafers of the hydrocarbons on the surface and leave just the native oxide (SiO_2) on the silicon substrate. I used the

apparent oxide thickness from the ellipsometer to know that I had an apparent oxide that matched the expected value of the native oxide at 1.8nm$\pm$0.03 nm and I used XPS to confirm that 1.8 nm corresponds with a significant decrease in the presence of carbon.

I used a variety of techniques to get the apparent oxide thickness to 1.8 nm. The technique varied depending on what the storage conditions for the sample had been. I always wore Latex Adenna Explorer gloves, samples were handled only with a specific set of tweezers and I was very careful never to breathe over the samples. I used these precautions because previous XPS measurements indicate that touching a surface with a gloved hand or worse, with a bare hand significantly increased the apparent oxide thickness [6].

I found that while the Evactron could clean the samples, the cleaning process took a lot longer than the other cleaning techniques I tried so it was not a process that I studied extensively. I also tried cleaning with a Harrick Plasma cleaner–a typical version of small-scale plasma cleaners that creates plasma from air much in the same way as the Evactron. Like the Evactron, I only cleaned a handful of samples with this technique. Through XPS data I found that a significant amount of fluorine was deposited onto the surface due to this process[1]. Thus, the cleaning techniques that I studied extensively were the RCA clean and the excimer lamp.

The Radio Corporation of America (RCA) clean is a two-step chemical process[2]. The first step is very basic (pH of 14) and is designed to remove organic film contamination via oxidative breakdown. Hydrogen peroxide (30%) and ammonium hydroxide (30%) are diluted in water in a 5:1:1 H_2O:H_2O_2:NH_4OH solution. This is heated to

[1] Since other users clean their samples with HF prior to using the Harrick, I attribute the fluorine presence to their samples

[2] The clean was developed by Werner Kern in 1965 while he was working for the Radio Corporation of America, and from that the name of the clean arises

$70 - 85\,^{\circ}\mathrm{C}$ and the sample is entirely submerged in the mixture for 10 minutes. At the requisit cleaning temperature, the solution is boiling and evaporates over time. It is important to ensure that there is enough to fully immerse the sample for the entire ten minutes. The samples become tremendously contaminated if the solution is allowed to evaporate off them. After the 10-minute first step, the sample is removed with teflon tweezers and is rinsed with de-ionized water and blown dry with nitrogen gas. The second step is very acidic (pH of 1) and is designed to remove alkali ions and cations that form NH_4OH-insoluble hydroxides in the first step. It is a mixture of hydrogen peroxide (30%) and hydrochloric acid (37%) in water with the ratios 6:1:1 H_2O:H_2O_2: HCl. It is also heated to $70 - 85\,^{\circ}\mathrm{C}$ and the sample is again immersed for 10 minutes whereupon it is rinsed and blown-dry as before. In the literature, there various optional additions to this two-step process have been studied for samples that were hugely contaminated (with a photoresist for, example). I did not explore any of the optional steps since they involved HF and it was highly probable that such treatment would etch the surface, contributing to surface roughness and doing far more damage to surface reflectivity than the original contamination would.

I used an xenon excimer lamp made by Resonance LTD to clean other samples with excimers arising from oxygen being bombarded with 7.2eV light. Although the lamp was cooled with nitrogen and operated in a hood, the sample itself was cleaned in air at ambient pressure. Samples were generally placed 1 cm from the lamp. Placement lower then that resulted in lower levels of cleanliness. The lamp's operating principle is to create excimers–molecules formed from at least two atoms with at least one of the atoms in an an excited state–that bind to the advenitious carbon. (A bi-product of the lamp is ozone, and it is for this reason that it is requisite to operate it under a hood.) I primarily studied optimal cleaning times with the lamp as well as what kinds of carbon bonds are most strongly attacked with the excimers.

Chapter 3

Results and Conclusion

As reported above, for the samples to have an apparent oxide thickness of 1.8 nm or less, the samples must be either cleaned with the excimer lamp for at least 5 minutes or go through both steps of the RCA clean. See Fig 3.1. The figure demonstrates the general cleaning trend: "mostly clean" samples need at least five minutes of UV irradiation exposure to return the sample surface to its native oxide. The mean apparent oxide thickness for these 45 five-minute samples is 1.83±0.03 nm (pictured as the white triangle) with only 15 of these samples measuring thicker than 1.83 nm. The two outliers at five minutes are somewhat puzzling. It is very possible that the sample with an apparent oxide thickness of 1.95 nm wasn't positioned directly under the lamp. Direct placement under the lamp is critical to the cleaning process (as is ensuring that the sample is placed within 1 cm of the lamp). The outlier on the other end is the sample that showed an apparent oxide of 1.76 nm. It happens that it was cleaned slightly differently from most of the other samples. The majority of the time, whenever the lamp was in operation the plasma source (a small component of the lamp) was cooled with nitrogen. However for several samples a nitrogen hose was attached to the lamp's box allowing nitrogen to flow through the entire instrument

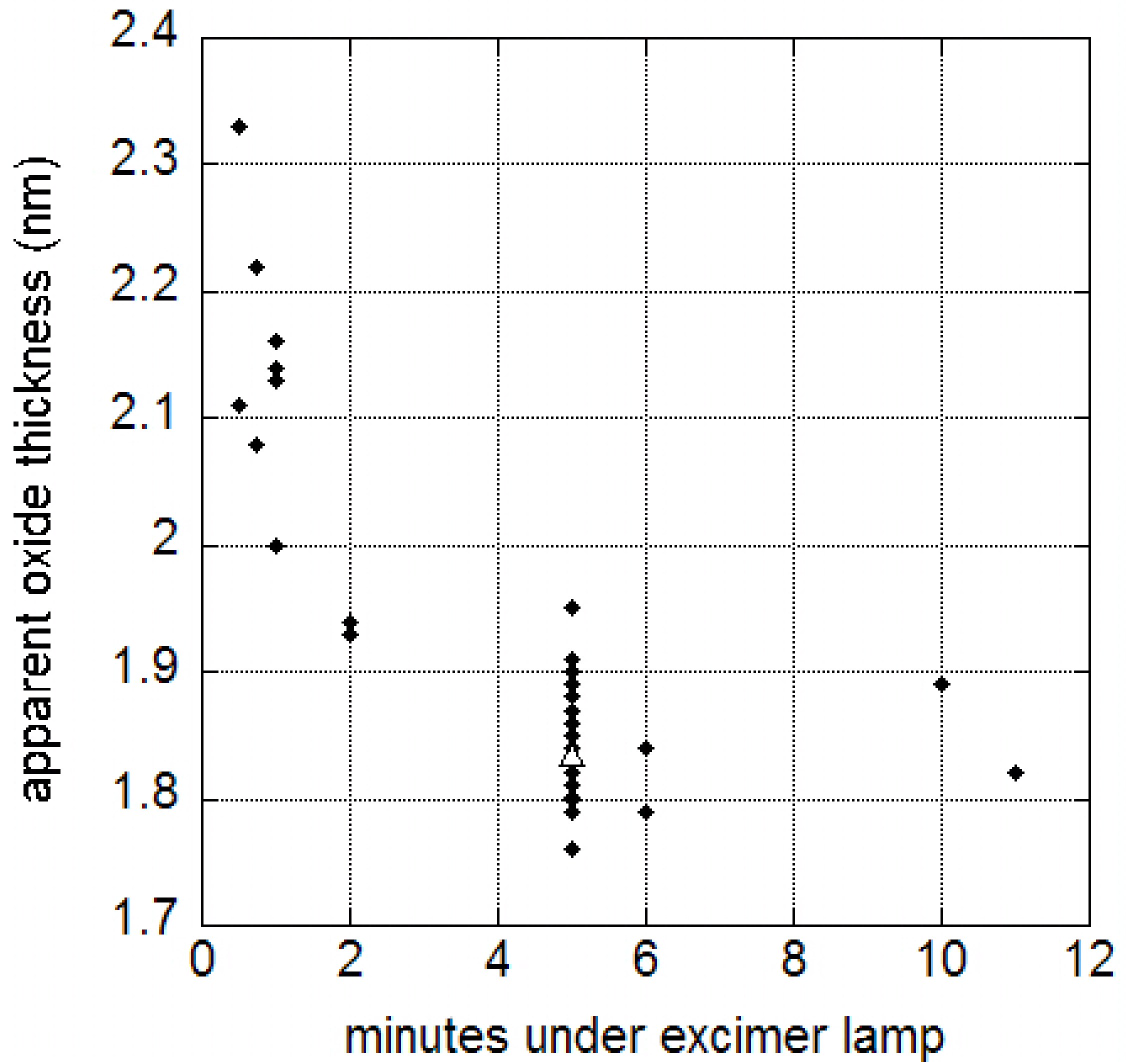

Figure 3.1 Decrease in the thickness of the apparent oxide layer vs UV exposure time. All of the data in this graph come from 59 samples that were cleaned exclusively with the excimer lamp. 45 samples were cleaned for five minutes. The white triangle on the graph represents the mean five-minute thickness. Of these 45 samples, 30 lie at or below the mean. There is clearly a trend in the data that supports the claim that 5 minutes under the lamp will take a nearly clean sample and decrease the apparent oxide thickness by several more angstroms.

rather than just cooling the small component. Even though the sample was cleaned slightly different from most of the other samples, this particular sample might just be an anomaly since several samples were cleaned under the same conditions and it was the only one to exhibit such a dramatic decrease in the apparent oxide thickness.

The data also show that optimal cleaning time varies somewhat from sample to sample. In general, the dirtier a sample, the more UV irradiation time it needs. To illustrate this point I will discuss my absolute dirtiest samples. They were created when I was experimenting with various storage options. I thought that perhaps the samples would remain free of carbon contamination if they were stored in a chemical medium rather than the lab air. I found that I was wrong and the process of varying the storage medium resulted in some very dirty samples. Six samples were first cleaned with the lamp to 1.83±0.01 nm and then submerged in a bath of isopropenal which was housed in glassware that I had prepared by washing it with methanol and blow drying with nitrogen. A week in storage showed that some of the isopropenal had evaporated and the apparent oxide layer for three of the samples had increased to 3.8±0.2 nm. After three weeks, the isopropenal completely evaporated and thanks to thin film interference, even a glancing visual inspection revealed that a film had deposited on the surface of these samples. With the standard "apparent oxide" model, these evaporated samples had an "apparent oxide" of 25-27 nm, but there was quite a large error on the fit, with an MSE of 10.2,[1] suggesting that for this much carbon, the carbon layer needs to be modeled directly. However, for the purposes of seeing the effect of the lamp on the sample, a qualitative description of the change in the

[1]A typical MSE for the ellipsometer is 1.8. A good fit was one with an MSE lower than 1.5. If after repeated measurements and trying at least two samples, the MSE wouldn't lower past 2.8, I would stop taking data and rigourously realign the instrument. If that failed to work, I would try turning everything off for awhile and then restart, making sure to allow the ellipsometer 20 minutes to warmup.

sample as measured by the ellipsometer was sufficient. For one of the dirty samples, a five minute exposure to the lamp caused the "apparent oxide" to decrease by 17 nm. Again, the measured thickness had a larger error with an MSE of 4.2 because it's not a good model. It decreased an additional 5.4 nm after an additional five minutes. The error on this final thickness was still high with an MSE of 3.7, but it's encouraging that the error decreases with thickness. These dirty samples provide dramatic illustration of the lamp's cleansing effect and demonstrate that the dirtier the sample, the more lamp exposure time it needs. Most of the samples I studied were not nearly so contaminated; however, I saw this same overall trend in all the samples I studied.

Accurate surface characterization demands the use of multiple techniques. Conclusive results arise when there is agreement in the results between these different techniques. In that spirit, one of the most important results of my research is that I demonstrated that there is a direct correlation between an increase in "apparent oxide thickness" (determined by ellipsometry) and an increase in the carbon(determined by XPS). See Fig. 3.2. The carbon concentration was determined by XPS measurements and normalized to the silicon concentration using an analysis package provided by Surface Physics. In the XPS survey scans I always saw peaks corresponding to carbon, oxygen, and silicon. XPS results are inherently relative so to report the data, I chose to compare carbon (which is the element of interest) to silicon. I chose this primarily because oxygen is more of a variable: in addition to being part of the SiO_2 layer, it is part of the adventitious carbon and so, like carbon, it changes with lamp exposure. The silicon concentration, however, remains constant during the UV irradiation process; consequently I generally normalized the carbon to the silicon[2].

[2] The only exceptions were the dirtiest samples discussed previously. The carbon layer on these samples was so thick that XPS failed to detect the presence of silicon on the surface. XPS penetration

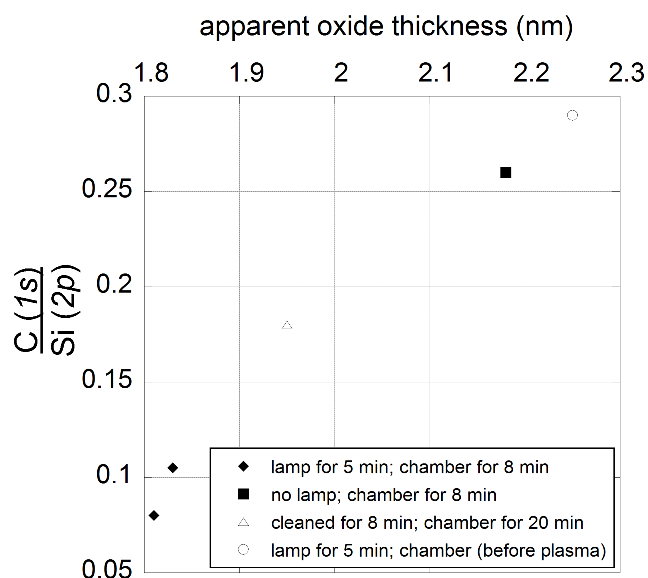

Figure 3.2 Correlation between the thickness of apparent oxide layer and the carbon concentration determined Data show agreement between the instrumental characterization techniques of ellipsometry and XPS.

The data for Fig. 3.2 come from samples exposed to a variety of conditions. Of particular interest is the data the show the difference between a UV irradiated sample and an untreated sample. The following results come from samples that were put into the XPS antechamber after it was plasma cleaned for about 45 minutes. They were inside the chamber for approximately eight minutes total in an attempt to minimize the carbon contamination from the chamber. Ellipsometry suggests that the apparent oxide changed by 0.8±0.03 nm. Despite the slight contamination the results demonstrate a distinct different between the two types of samples. An untreated sample with an apparent oxide thickness of 2.17±0.02 nm gives the carbon concentration to be 26.2% carbon to 73.8% silicon. A sample exposed to the lamp has an apparent oxide thickness of 1.81±0.03 nm and 8.4% carbon to 91.6% silicon. (See Fig. 3.4a

depth is somewhat of a variable, but in general we assume that it sees about 5 nm into a surface [7]. The XPS data from the dirtiest samples suggest that 5 nm is approximately correct: for one of the dirty samples the ellipsometer's rough assessment of the "apparent oxide" was 5.4 nm and the corresponding XPS data for that thickness was unable to detect silicon

and Fig. 3.4b)

As long as the contamination from the antechamber was minimized with the Evactron, all samples showed that the C (*1s*) peak significantly decreases relative to the silicon peak for samples exposed to the excimer lamp for at least 5 minutes. The peak fitting and line shape analysis of the C (*1s*) peak reveals how the excimer lamp's cleaning treatment affects the adventitious carbon [8] on the sample surface (see fig. 5). I fit the data using a Shirley background and the peak fitting package supplied by Surface Physics. To provide statistical analysis of the peak fit, I used the Mathmatica 6.0 fitting package and fit the data to Gaussian and Lorentzian models. The Gaussian was chosen to model the experimental aspect of the measurement (the instrumental response, x-ray line-shape, Doppler broadening) and the Lorentzian to model the broadening due to the uncertainty principle in the energy and lifetime of the ejected electrons. Peak fitting the carbon peak on a dirty sample suggests that C-H or carbon-only type bonds are the dominate feature. There is always some partially oxidized adventitious carbon present (As discussed previously, it was for this reason that carbon concentrations were normalized to the silicon rather than to the oxygen). Cleaning with the lamp significantly decreases the carbon-only AC and the oxidized carbon. (See Fig. 3.6)

Like cleaning with the lamp, an effective RCA clean effectively eliminates adventitious carbon contamination. The carbon to silicon ratios are comparable to those of the lamp. The apparent oxide thickness after the RCA clean generally falls between 1.5-1.8 nm, which is less than what the lamp gets it to. But since the ratios of carbon to silicon are about the same, the thinner apparent oxide thickness suggests that rather than entirely eliminating carbon, the RCA clean eventually begins to attack the oxide layer on the silicon. It could also well be that the carbon detected in by XPS is not left by the cleaning, but rather deposited on the surface by the antecham-

Figure 3.3

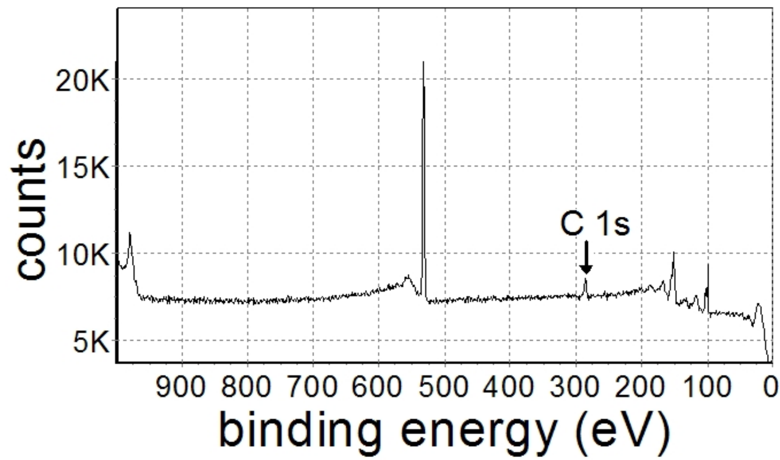

(a) Survey scans for untreated wafers show a distinct carbon peak. Note the small peak labeled C *1s* here at about 285 eV is missing in fig. 3.4b

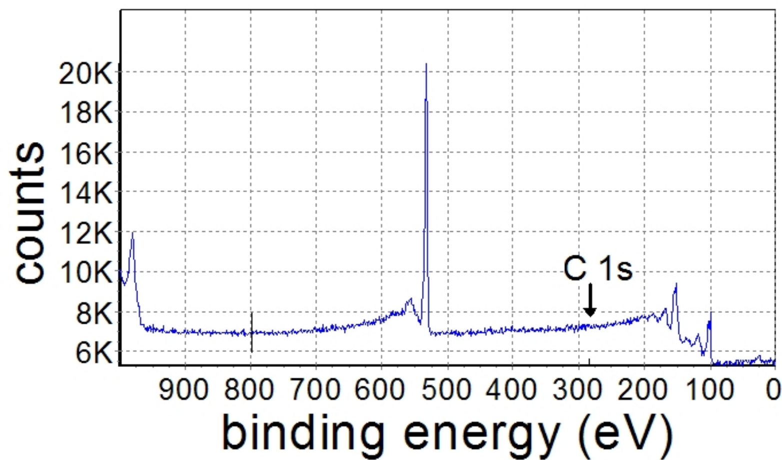

(b) There is no distinct carbon peak at 285 eV in the survey scans for the wafers exposed to excimer lamp irradiation for 5 minutes

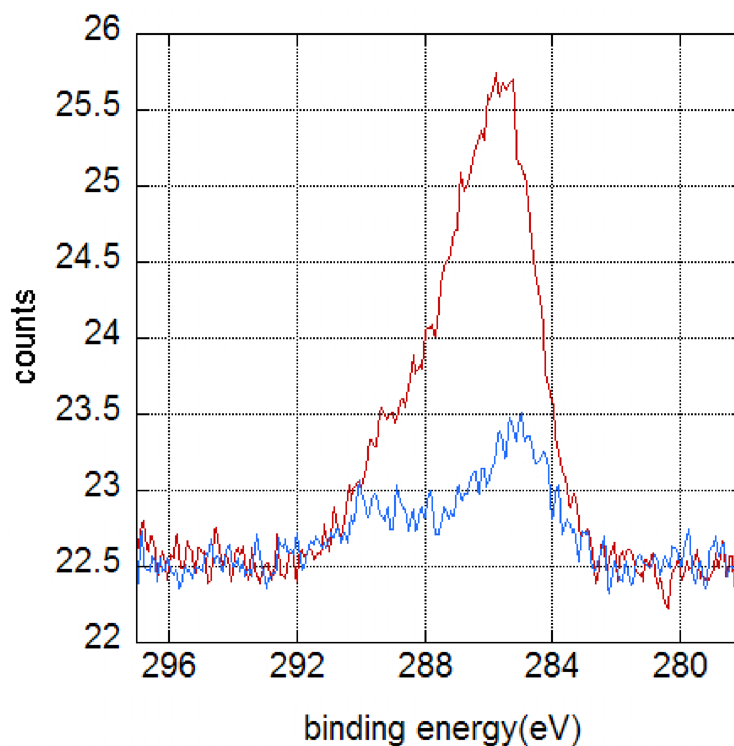

Figure 3.4 The red line corresponds with a dirty sample while the blue line corresponds with a sample cleaned with the excimer lamp.

ber. I haven't been able to conclusively determine which is the case. Thanks to the Evactron, the apparent oxide thickness no longer grows during a 10-20 minute exposure to the antechamber–it either stays the same or decreases slightly. But since at this level the carbon contamination is so slight, I don't feel justified in dismissing the chamber as a potential source of contamination despite the readings from the ellipsometer. From a practical standpoint it is more challenging to control the RCA clean and presumably this explains why there is such a range in the apparent oxide thickness for the RCA cleaned samples. Furthermore, the cleaning technique worked the majority of the time, but twice the apparent oxide thickness went down while the carbon levels stayed high on the RCA cleaned samples (and decreased for lamp-cleaned samples). It also occasionally appears to deposit trace amounts of lead and iron onto the surface. Since the samples were cleaned in a shared chemistry lab, it is

Figure 3.5

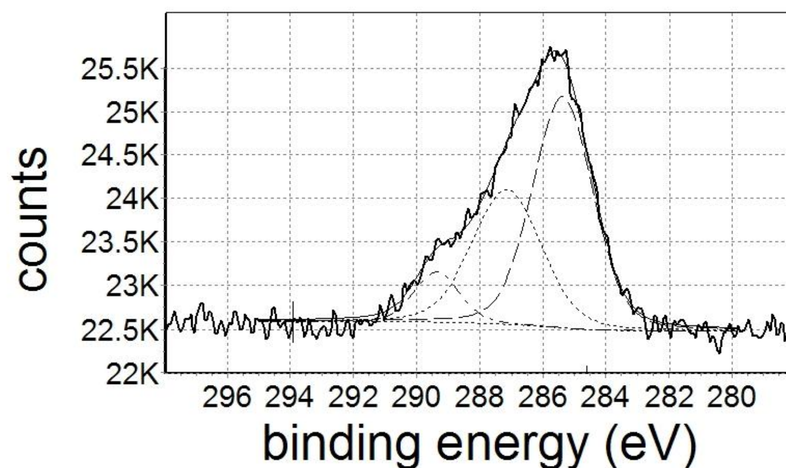

(a) C (*1s*) peak for untreated wafers show higher levels of adventitious carbon contamination. From the peak fit for this sample we see that the carbon-only type bonds are the dominate feature. We also see two statistically significant peaks of the OC type.

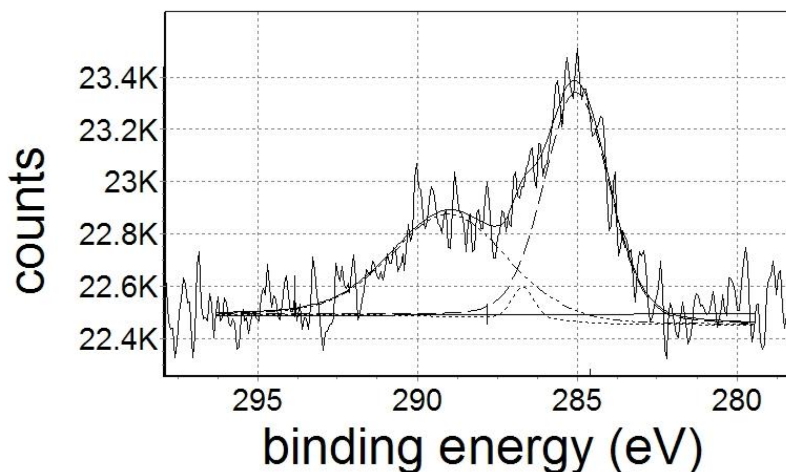

(b) C (*1s*) peak for wafers exposed to the excimer lamp. The carbon peak is not as distinct. Statistically speaking, the peak fit only recognizes the carbon-only peak and one peak of the OC type.

Figure 3.6

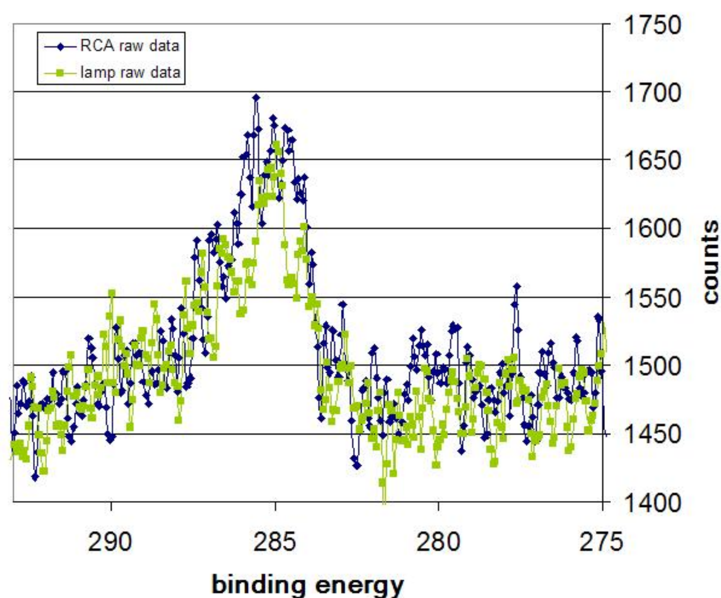

Figure 3.7 Compares the raw data for the carbon peaks measured by XPS for samples cleaned with the RCA clean to those cleaned with the lamp.

possible that these defects are due the to lab conditions, but in the literature others reported seeing iron on the surface as well [9]. (They suggested removal with a brief rinse in HF.)

One more thing remains to be discussed: the conclusions from the storage study. I begin by describe the sample set analyzed. Additionally I studied the immediate effects of contamination redeposition following the RCA cleaning treatment. From the data I can make the following conclusions. Typically with nonvacuum storage conditions, after two hours of being cleaned by any method, 0.1 to 0.2 nm of hydrocarbon reappear on the surface (see fig. 3.8).

A total of 85 samples were stored and 208 data points were taken from these samples. Statistical studies were preformed on the data using the regression tool in Excel, the ANOVA package in Kaliograph and the R^2 software package. The various statistical studies all provided similar results. Data was studied in two different sets: one data set included all 208 data points while the other included only 75 points.

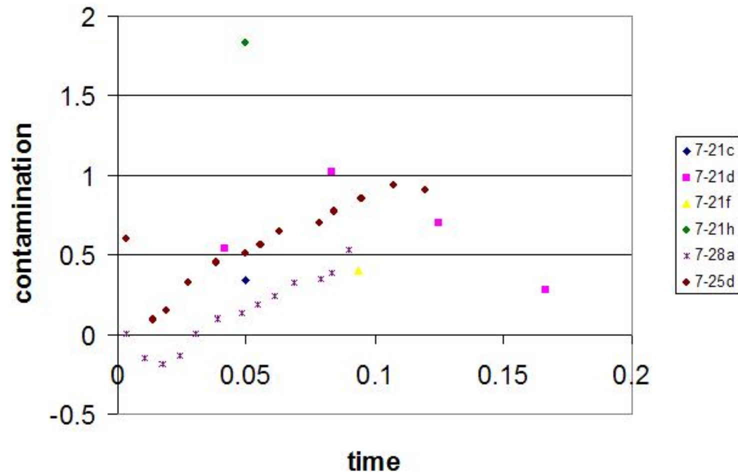

Figure 3.8 Tracks change in the apparent oxide thickness immediately after being cleaned with the RCA lamp. The data from Sample 7-21d are somewhat misleading because the sample was analyzed in all different spots. Samples 7-28a and 7-25d where measured in the same spot, and the data are more meaningful.

This was done because I found that two samples cleaned at the same time, from the same wafer the same apparent oxide thickness would have different amounts of contamination on them over time if I measured one more than the other. This finding makes sense since in measuring the samples, since I had to remove them from storage and thus change their storage conditions. By looking at all 208 data points, there is more data collected for the samples with repeated measurements thus the data set is skewed to favor the more contaminated samples. In an effort to adjust for this effect while still maintaining a spread of measured time, I created a random number generator and randomly selected one data point per sample, creating the second set with 75 data points (10 samples either had slightly ambiguous inital starting data or a confusing storage history, so I chose not to include them in the select set). From these sets I used the aforementioned packages to analyze the data.

The statistical analysis says that initially the two factors that matter the most are time stored and the manner in which the sample was clean. Incidentally, most of the contamination growth occurs immediately after cleaning (regardless of the method).

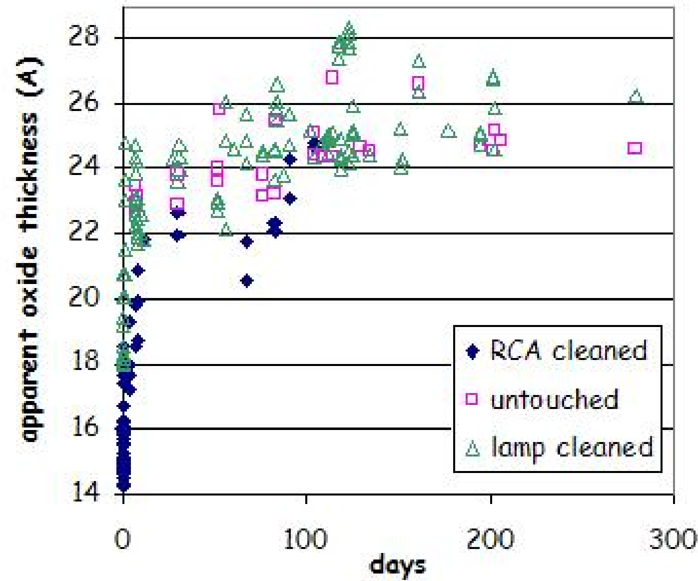

Figure 3.9 Measured apparent oxide thickness vs time. This storage data comes from 85 samples with a total of 208 measurements. Storage time varied from ten minutes to 279 days. Although the starting apparent oxide thicknesses varied over a 1 nm range, the data show that the samples accumulate similar amount of avenitious carbon contamination over time.

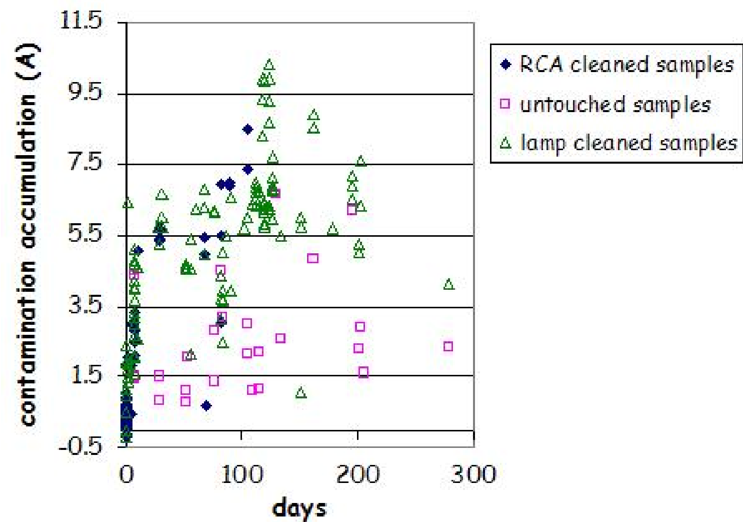

Figure 3.10 Change in apparent oxide thickness vs time. This storage data comes from 85 samples with a total of 208 measurements. Storage time varied from ten minutes to 279 days. This demonstrates how that contamination accumulation growth is different from samples that were never exposed to a cleaning technique.

For long term storage, the storage location and initial contamination become statistically significant (see fig 3.9). Whether or not the sample was cleaned also slightly affects contamination accumulation. Cleaned samples generally collected slightly more than their accompanying untouched "control" samples; furthermore, some of the untouched samples experienced extraordinarily low contamination accumulation (see fig. 3.10). It is therefore, instructive to look at the change in contamination which is determined by subtracting the stored value for the apparent oxide thickness from the initial measured apparent oxide thickness value. However, looking at the change only can distort the data. It is, therefore, also instructive to study variations in the total measured apparent oxide thickness. Compare figures 3.9and 3.10. The conclusions from the statistical study are that the two most important factors in determining the total expected amount of contamination over the long time is (1)the time it was stored and (2)how much contamination it originally started out with.

Bibliography

[1] B. L. Henke, E. M. Gullikson, and J. C. Davis, "X-ray interactions: photoabsorption, scattering, transmission, and reflection at E=50-30000 eV, Z=1-92," Atomic Data and Nuclear Data Tables 77 (1995).

[2] E. Gullikson, "X-Ray Interactions With Matter," .

[3] J. Tveekrem, "Contamination effects on EUV optics," NASA Technical Report TP-1999-209264 (1999).

[4] N. Farnsworth, "Thorium-based Mirrors in the Extreme UltraViolet," Honors Thesis (Brigham Young University, Provo, UT, 2005).

[5] P. Tripathi, G. S. Lodha, M. H. Modi, A. K. Sinha, K. J. S. Sawhney, and R. Nandedkar, "Optical constants of silicon and silicon dioxide using soft X-ray reflectance measurements," Optics Communications **211,** 215–223 (2002).

[6] R. E. Robinson, R. L. Sandberg, D. D. Allred, A. L. Jackson, J. E. Johnson, W. Evans, T. Doughty, A. E. Baker, K. Adamson, and A. Jacquier, "Removing Surface Contaminants from Silicon Wafers to Facilitate EUV Optical Characterization," In *47th Annual Technical Conference Proceedings (SVU-Tech Dallas, TX, April 2004)*, **47,** 368–376 (Society of Vacuum Coaters, Albuquerque, NM, 2004).

[7] A. Grigg, "Oxidation effects of the optical constatns of heavy metals in the extreme ultraviolet," Honors Thesis (Brigham Young University, Provo, UT, 2007).

[8] T. Barr and S. Seal, "Nature of the use of adventitious carbon as a bind energy standard," J. Vac. Sci. Technol. **A,** 1239–1246 (1995).

[9] W. Kern, "The evolution of Silicon Wafer Technology," J. Electrochem. Soc. **137,** 1887–1892 (1990).

[10] R. Azzam and N. Bashara, *Ellipsometry and Polarized Light* (North-Holland Publishing Company, Amserdam,NY, 1977).

[11] J. Peatross and M. Ware, *Physics of Light and Optics* (Brigham Young University, Provo, UT, 2007), pp. 56,88.

[12] C. Herzinger, P. Snyder, B. Johs, and J. Woollam, "InP optical constants between 0.75 and 5.0 eV determined by variable-angle spectroscopic ellipsometry," 54 (1995).

[13] J. Taylor, *An Introduction to Error Analysis: The Study of Uncertainties in Physical Measurements*, 2nd ed ed.

[14] W. P. nd B.P Flannery, S. Teukolsky, and W. Vetterling, *Numerical Recipes: The Art of Scientific Computing* (Cambridge University Press, Cambridge,MA, 1988).

[15] E. Pallik, *Handbook of Optical Constants of Solids*

Appendix A

Ellipsometry

Scientists have all sorts of ways of probing things. One way is to observe how something changes as a result of interacting with whatever it is that you're trying to characterize. This method is particularly useful when the change is (1)quantifiable and (2)material dependent. Ellipsometry fits the bill in both regards. The basic idea is to detect how the light changes when it interacts with some material and then use that data to distguish differences between samples. Data from the ellipsometer can be used in conjuction with other characterization methods to determine absolute thicknesses and optical constants (n and k). They can also be used to relative determinations of the differences between samples.

Ellipsometry takes advantage of how polarization changes when a light wave interacts with a new medium. This change occurs because the parallel and perpendicular components of light don't reflect from the boundary the same way [10].

The Fresnel coefficients are incredibly useful numbers that give the ratio of the reflected and transmitted field and they are broken down in terms of s and p polarization (that means you have a Fresnel coefficient for the reflected s-polarized light and a different one for the reflected p-polarized light). Each time the light encounters a

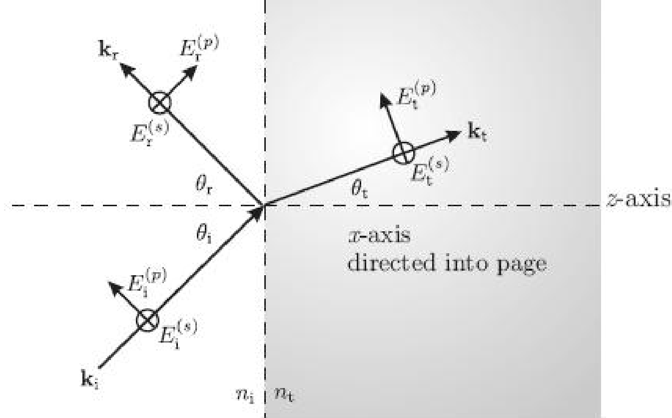

Figure A.1 When light is reflected from a boundary the s-polarized light stays the same, while the p-polarized light flips to match the direction of wave propagation [11].

new medium, new values for the respective Fresnel coefficients arise. The ellipsometer has light that interacts first with a controlled polarizer, then with the sample then with a variable polarization analyzer[1] and finally is collected with a photodetector.

So let's talk about light . . . and think about what things we could measure as we observe the light reflect off of something. Light is made up of electric and magnetic waves. And two good ways to pin down details of a wave (aside from determining how fast it's propagating, which is c in the case of light) is to measure its amplitude and its phase. The ellipsometer indirectly measures changes in these variables as light encounters a new medium. One slightly confusing point stems from what-the-blast the ellipsometer actually measures. It measures the "ellipsometric angles" psi and delta . . . two quanities that are pretty abstract but ultimately use ratios between the s and p components of the light to detect the differences in amplitude and phase as these two components interact with the surface of the sample.

If we start from square one, we should start with what the ellipsometer knows:

[1]The angle of the analyzing polarizer rotates at a high speed and the time dependence of the light reaching the detector is analyzed and correlated with the polarizer orientation [11].

it knows the initial polarization of the light it shines onto the surface. It's not a big jump for us to say that the E-field of reflected light is related to the E-field from the incident light. We relate it in the following manner

$$\mathbf{E}_r = \mathbf{R}\ \mathbf{E}_i \tag{A.1}$$

where **R** in a Jones matrix that describes the effect of the boundary on the light and establishes the relationship between the original E-field and the reflected E-field.

$$\mathbf{R} = \begin{vmatrix} |\mathbf{R}_{pp}|e^{i\delta_{pp}} & 0 \\ 0 & |\mathbf{R}_{ss}|e^{i\delta_{ss}} \end{vmatrix}$$

Here $|\mathbf{R}|$ quantifies the amplitude and δ quantifies the phase and the subscript "pp" goes with p-polarized light while "ss" relates to the s-polarized light.

As the ellipsometer measures polarization changes, it essentially is able to measure the ratio of the reflection coefficients in **R** as is seen in the following equation.

$$\frac{|\mathbf{R}_{pp}|}{|\mathbf{R}_{ss}|}e^{i\delta_{pp}-\delta_{ss}} = \rho = tan\psi e^{i\Delta} \tag{A.2}$$

The value ρ is a significant value not only because it can be calculated from the ellipsometer's measurements but also because it is a quantity that we can calculate using a theoretical model of the system. BYU's ellipsometer uses a software package called WAVES designed by the J.A. Woollam company. An outline for how the modeling portion of the package works is laid out in an article in the Journal of Applied Physics [12]. For the purposes of practical experimental use, creating the model is a matter of building a stack that describes the layers of thin films on the sample. After an initial fit, the model can be modified to include roughness, gradients in the layers, etc. Since this thesis concerns a two-layer stack of SiO_2 on Si, the following is for a two-layer system [2] When the light *first* interacts with the SiO_2, part of it is reflected and part of it is refracted (see Fig. A.2). The part that is refracted goes on

[2]If you care to expand to a model with more layers, chapter 4 of Azzam [10] does a rigorous

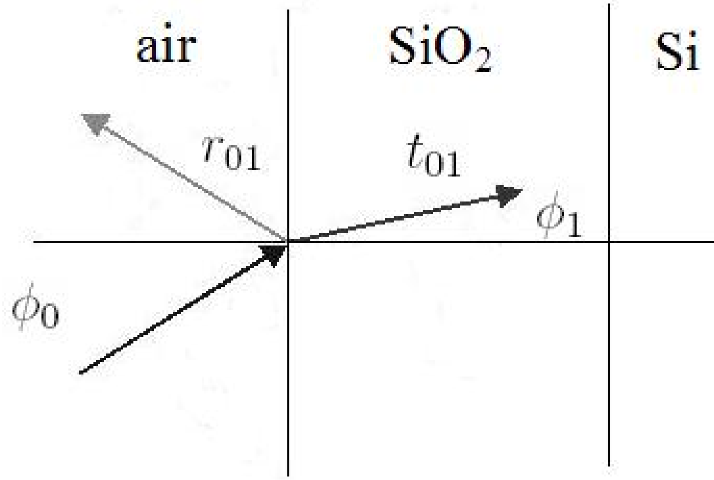

Figure A.2

to the Si barrier where again part of it is reflected and part of it is refracted. Take a second to note the notation on the Fresnel coefficients that I'm using in figure A.2: "r_{01}" is the Fresnel coefficient corresponding to reflected light at the SiO_2 boundary, therefore "r_{12}" corresponds with reflection at the Si boundary. The Fresnel reflection coefficients are given in terms of s and p polarization are defined with the following two general equations:

$$r_{(\alpha\gamma)p} = \frac{N_\gamma cos\phi_\alpha - N_\alpha cos\phi_\gamma}{N_\gamma cos\phi_\alpha + N_\alpha cos\phi_\gamma} \tag{A.3}$$

$$r_{(\alpha\gamma)s} = \frac{N_\alpha cos\phi_\alpha - N_\gamma cos\phi_\gamma}{N_\alpha cos\phi_\alpha + N_\gamma cos\phi_\gamma} \tag{A.4}$$

The light can bounce around inside the film many times before it is either absorbed by the Si layer or transmitted into the air. However, since the two boundaries are **not** perfectly reflecting, over time this internal wave loses energy. We need to take

job. Just make sure that you realize that he uses the engineering convention where $\mathbf{E} = E_0 e^{j(\omega t - kx)}$ instead of the physics convention where $\mathbf{E} = E_0 e^{i(kx-\omega t)}$. Or you can look at 6.8 of the BYU Optics Textbook [11] if you prefer manipulating E-fields rather than the fresnel coefficients. If you care to see the original work on reflectance in a two stack system, first learn to read German and then consult Drude.

this energy loss into account. The way that we do is to apply a decaying exponential that includes a term that considers both the properties of the material (in this case, SiO_2), and also the energy (or wavelength) of the light. In the literature this term is referred to as the film phase thickness and is given by

$$\beta = 2\pi \frac{d}{\lambda} N_1 cos\phi_1 \tag{A.5}$$

This film phase thickness is of particular importance to us because it includes the film thickness variable "d" which happens to be the variable we are ultimately interested in determining. The ellipsometer measures the total reflection.

We can use the stack-model to calculate what this total reflection ought to be. From the model, the first component of the reflected wave is the reflected light pictured in figure A.2 and given by the r_{01} term. The next comes from light that is transmitted into the SiO_2, reflects off the Si and then is transmitted back through the SiO_2. This is given by the term $t_{01}t_{10}r_{12}e^{i2\beta}$. To get the overall reflection of the light we add up all the "partial" waves that describe all the possible ways the light could reflect:

$$\mathbf{R} = r_{01} + t_{01}t_{10}r_{12}e^{i2\beta} + t_{01}t_{10}r_{10}r_{12}^2e^{i4\beta} + t_{01}t_{10}r_{10}^2r_{12}^3e^{i6\beta} + ..., \tag{A.6}$$

This looks like a mess, but if you realize that it's a geometric series and apply the general formula for a geometric series, it simplifies to

$$\mathbf{R} = r_{01} + \frac{t_{01}t_{12}r_{12}e^{i2\beta}}{1 + r_{01}r_{02}^2e^{i2\beta}} \tag{A.7}$$

The other thing we can do to clean this up is to note that if you where to somehow shine the light from inside the silicon (which is analogous to when the light travels back after it reflects off the silicon substrate) the new reflection and transmission coefficients are related to the "air based" reflection and transmission coefficients with

the following two equations[3]

$$r_{10} = -r_{01} \tag{A.8}$$

$$t_{10} = \frac{(1 - r_{01}^2)}{t_{01}} \tag{A.9}$$

By substituting these puppies into eq. A.7 out pops

$$\mathbf{R} = \frac{r_{01} + r_{12}e^{i2\beta}}{1 + r_{01}r_{12}e^{i2\beta}} \tag{A.10}$$

Now recall the equation for ρ (eq. A.11). On the one hand, it can be calculated from the values for ψ and Δ–the values measured by ellipsometry. On the other hand it can be calculated by knowing the ratio of the s and p polarized reflectances; and with eq. A.10 we have a way to calculate these reflectances using values that come directly from the two layer model we built. Thus,

$$\rho = tan\psi e^{i\Delta} = \frac{\mathbf{R}_{pp}}{\mathbf{R}_{ss}} = \frac{r_{01p} + r_{12p}e^{i2\beta}}{1 + r_{01p}r_{12p}e^{i2\beta}} \times \frac{1 + r_{01s}r_{12s}e^{i2\beta}}{r_{01s} + r_{12s}e^{i2\beta}} \tag{A.11}$$

This relationship is golden. It is (more-or-less) what the ellipsometer uses when its doing it's fit. According to the paper on ellipsometry modeling, they use the Levenberg-Marquardt algorithm in their fitting by minimizing the following equation

$$\xi^2 = \frac{1}{2N - M} \sum_{i=1}^{N} \left[\left(\frac{\psi_i^{mod} - \psi_i^{exp}}{\sigma_{\psi,i}^{exp}} \right)^2 + \left(\frac{\Delta_i^{mod} - \Delta_i^{exp}}{\sigma_{\Delta,i}^{exp}} \right)^2 \right] \tag{A.12}$$

Which is equivalent to minimizing

$$\xi^2 = \sum_{i=1}^{N} \frac{(\rho_{mod} - \rho_{exp})^2}{\sigma_i^2} \tag{A.13}$$

or

$$MSE = \frac{1}{n - f}\xi^2 \tag{A.14}$$

Where the "n" stands for the number of measurements, "f" stands for the number of fit parameters, and "MSE" stands for the mean squared error. The σ value in eq.

[3] You can prove these changing N_0 for N_1 in the standard Fresnel equations.

A.13 is the uncertainty in the measured ρ. This value can be found in the following manner [13]

$$\sigma_i = \sqrt{\left(\frac{\partial\sigma}{\partial\psi}\sigma_{\psi_i}\right)^2 + \left(\frac{\partial\sigma}{\partial\Delta}\sigma_{\Delta_i}\right)^2} \tag{A.15}$$

So, with all the pieces in place, the general idea is to adjust the parameters in the model until the model is as close as possible to the value the data calculate. Levenberg-Marquardt is an iterative process that uses nonlinear regression to fit multiple parameters[4]. To minimize ξ^2 take the derivative with respect to each parameter. The partial derivatives form a set of equations that can be adjusted iteratively until they are all simultaneously as close to zero as possible. In the case of fitting for thickness, the Levenberg-Marquardt technique is overkill since there is only one parameter that needs to be fit. A good initial guess and the “fminsearch command” in matlab are sufficient to determine what thickness is best to minimize ξ^2. (Use of Levenberg-Marquardt is needed if ellipsometric data is being used to determine optical constants rather than thickness.)

On a practical note, when BYU’s ellipsometer takes data, it reports all the values needed in order to minimize ξ^2 in matlab. In other words, it tracks ψ, Δ, the uncertainties in these constants along with the tables of optical constants it uses in it’s fitting[5] When using the instrument, it is important to use multiple angles around Brewster’s angle. At Brewster’s angle there is the largest difference in reflection between the s and p polarized light. For the p-polarized light at Brewster’s angle, which incidentally is defined as $tan\phi_B = \frac{n_1}{n_2}$, there is a phase shift at the boundary and correspondingly the amplitude of the reflected light must be zero. For the s-polarized

[4]This Levenberg-Marquardt process is absolutely brilliant and an outstanding explanation for how it works can be found in chapter 14 of Numerical Recipes: The Art of Scientific Computing [14]

[5]Some of these optical constants come from Pallik [15], and some appear to come from their own measurements.

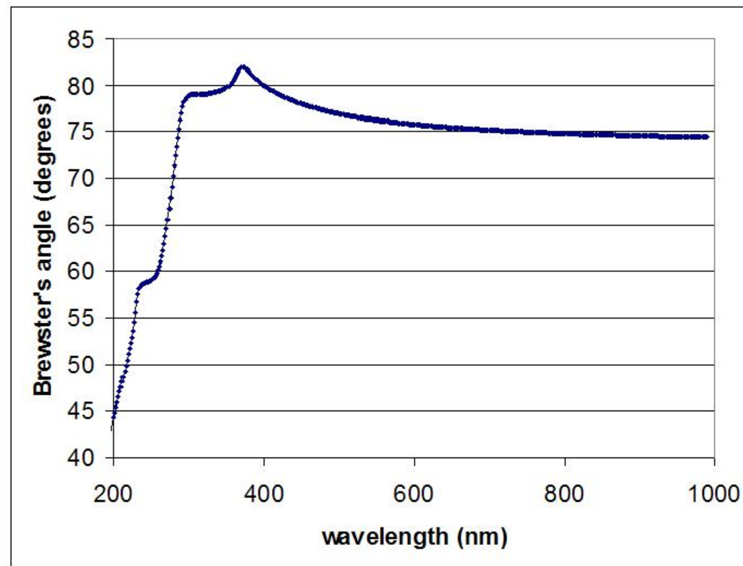

Figure A.3 variation in Brewster's angle for silicon for the wavelengths measured with the ellipsometer.

light, there is no phase shift at the boundary and the amplitude of reflection simply continues to increase. Thus, the ratios measured by the ellipsometer are the most distinct around Brewster's angle. Since n and k vary with wavelength, brewster's angle also varies over the range (see fig. A.3) however for about two thirds of the wavelengths, the angle is very close to 75 °. Thus I chose to measure thickness with the following five angles: 70 °, 72 °, 74 °, 76 °,and 78 °. (The multiple angles are helpful in creating an independent system of equations when we go to minimize ξ^2, although by way of cautionary note, please realize that just adding angles won't always provide data to help minimize ξ^2. If on preforming a parameter correlation test, you find that the measurements are interdependent then you haven't actually provided additional data by measuring multiple angles.)

Finally, I have two more practical bits of advice. The first is to let the ellipsometer warm up for 10-20 minutes before using it. Why it needs this long, I'm not sure. I do know, however, that it doesn't give reproducible data for the first little bit that it's turned on. The second thing is to realize that a sample with a uniformly thick film

is the exception rather than the rule–the larger the sample, the more measurements (in different spots) need to be made. For this reason I tended to cut relatively small samples.